Chapter

Application of a Frequency-Based Detection Method for Evaluating Damaged Concrete Sleepers

Kodai Matsuoka and Tsutomu Watanabe

Abstract

Frequency-based damage detection (FDD) has been studied for a long time. Generally, it is pointed out that FDD is less sensitive to detect the damage in civil structures, which are composed of many members precisely. However, for the structural members on the premise of replacement like concrete sleepers, the FDD approach that has been accumulated so far may be effective. In addition, its ease and simplicity of the system are an advantage of realizing regularly and inexpensive inspection on the sites. Here we introduce the damage influence on the concrete sleepers based on the laboratory tests and demonstration of the practical use of FDD through some filed tests.

Keywords: concrete sleeper, frequency, damage detection, field test

1. Introduction

A railway prestressed concrete sleeper is one of the important components supporting rails and distributing train axle loads into ballast [1]. Mono-block type concrete sleepers, one of the most common sleeper types, are conventionally used in countries such as Australia, Canada, China, Italy, the UK, the USA, and Japan [2]. In Japan, a large number of these sleepers have been continuously introduced into railway lines since the 1950s [3], with some exceeding 50 years of operational lifetime. Thus, sound methodologies and tools for achieving effective maintenance of such a vast number of concrete sleepers are ultimately required [4].

An impact axle load is a typical scenario that can promote cracks and influence the deterioration of concrete sleepers [5–9]. In particular, some impact loads due to wheel irregularities (e.g., flat wheels), rail irregularities, and rail joints would likely over time produce concrete cracks at the bottom of rail seats and at the top of midspans where the maximum or minimum bending moment arises as shown in **Figure 1** [3, 7]. A low-occurrence probability of such significant loads acting upon concrete sleepers actually exists; however, when they do occur, yielding of steel members, residual displacement, and/or open cracking of surrounding concrete will often result. Open cracking allows water to penetrate into the sleeper ultimately causing corrosion of reinforced steel, which then leads to a loss in bending strength [8].

Currently in Japan, the inspection of concrete sleeper deterioration/damage is typically carried out by visual inspection via foot patrol. However, concrete sleeper bodies, with the exclusion of their top surfaces, are usually covered by ballast (as shown in **Figure 1**). It is therefore difficult, in general, to detect damage by visual inspection.

Even if the ballast around sleepers is scraped out, damage such as cracks cannot always be detected due to the clogging of cracks with soil dust. Moreover, scraping out ballast to inspect sleeper states is not realistic due to the enormous number of concrete sleepers that require inspection. Vibration-based structural damage detection, however, is a potential method that may be employed for effectively remedying this challenge.

Vibration-based structural damage detection is a well-known concept and widely invoked within the domain of structural health monitoring [10, 11]. For civil engineered structures, many researchers and engineers have performed such related assessments [12, 13]. Thus far, varying degrees of success for state evaluations of actual structures focusing on local and higher vibration modes and vibration characteristic changes before and after earthquakes have been reported [14–16]. In contrast, however, substantial numbers of structural damage occurrences have been detected impractically, thereby resulting in general detection methodologies that do not specifically focus on actual structural systems or accrued associated damage thereof. Assuming a damage detection method for practical applications, however, characteristics of target structure types and their typically incurred damage modes should be investigated. From this point of view, an advanced methodology is not always required but rather typically depends on characteristics of the target structure.

Concrete sleepers typically display a characteristic in which a singularly damaged sleeper does not usually prompt a major impact on train-running safety or riding-comfort provided they can transmit trainloads and retain a gage [3]. Only in instances of multiple and consecutive concrete sleepers maintaining serious damage levels are the potential impacts on safety or comfort. This means that a state evaluation method based on continuous monitoring or advanced detection techniques is not necessary for concrete sleepers. If one can ascertain whether or not a measured concrete sleeper needs replacement, it could sufficiently contribute to the achievement of an effective maintenance protocol for them even if the utilized detection methodology is widely regarded as antiquated.

Several related references have previously pointed out the possibility of detecting concrete sleeper damage based on measured modal characteristics. Lam et al. [17, 18] and Kaewunruen and Remennikov [19, 20] developed ballast damage detection methods using the natural frequency and mode shape of in-situ concrete sleepers. In those studies, frequency-based damage detection for concrete sleepers was described as "an important future task". In addition, Kaewunruen and Remennikov [21] investigated the effects of rail pad stiffness on the modal parameters of sleepers, and Matsuoka et al. also investigated the modal properties of damaged sleepers [22]. Despite these contributions, the overall feasibility of the damaged-sleeper detection process remains uncertain because of the absence of the following three critical factors: impact of

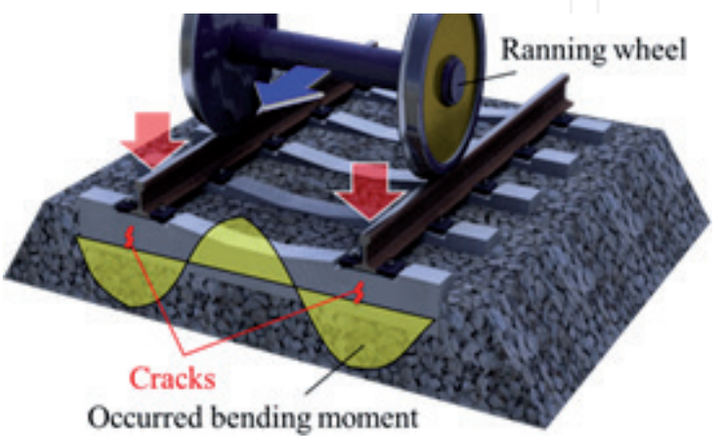

Figure 1.
Illustration of concrete sleeper installations and typical bending moment distribution during train passage.

concrete sleeper damage on modal characteristics, influences of specification variations of other track members, and a simple and efficient measurement process for practical use. An important contribution of this study is the provision of valuable data relating to impacts of typical damage modes, such as cracks and steel rod fractures, on the modal characteristics of general concrete sleepers in Japanese railway. Another contribution of this study is to propose a simple and efficient detection method assuming a practical application. As for vibration measurement methods of concrete sleepers, they have not been investigated other than via the use of accelerometers [19]. It is, however, difficult to apply such practical uses in which more than several tens of thousands of sleepers would require inspection per a rail line. This study therefore focuses on a detection method based on a hammering sound with a well-known impulse hammer technique to improve detection efficiency by omitting the installation of accelerometers.

2. Experimental methods

In this research, in order to verify the proposed damage detection system, several experiment series were set up, and necessary concrete sleepers were collected for each experiment. First series are new concrete sleepers. These are used to investigate the relationship between damage and mode characteristics through the stepwise bending test. These are also used to evaluate the influence of other track members (i.e., pad stiffness and ballast-supporting stiffness) on modal characteristics of sleepers on the actual environmental tests. Second series are concrete sleepers with actual damaged. Comparative studies of these concrete sleepers can provide an empirical validation of the feasibility of vibration-based damaged-sleeper detection. In addition, measurements using both accelerometers and sound-level meters were ultimately performed; comparison of such results can provide substantive evidence of applicability for the effectiveness of the sound-based detection method.

2.1 Test concrete sleepers

Figure 2 and **Table 1** provide design drawings and nominal specifications of test sleepers in this research endeavor. Specifically, this study focuses on 3PR and 3PO sleepers which are the most widely used types of sleepers on meter-gauged railway lines in Japan. 3PR/3PO are pre/posttension and mass/individual-production types, respectively. Posttensioning types utilize an unbonded system in which the steel-concrete bond is removed by an asphalt-based resin material.

Table 2 provides a list of test concrete sleepers. Six pretension and seven posttension type sleepers, which had been previously used in actual railway lines in Japan, were collected. Sleeper Nos. 1 and 9 shown as intact in **Table 2** were given artificial damage by stepwise bending tests, with vibration measurements. Sleeper Nos. 2–5 and 11–14 had different degrees of cracking or steel rod fractures generated through actual operational history. **Table 2** also presents these damage levels as "cracked sketches." Sleeper Nos. 6 and 13 are destroyed sleepers resulting from bending tests, in order to evaluate excessively damaged sleeper states. Other vibration measurements in a full-scale test line (described later) were performed on six intact sleepers (Nos. 17–22). In contrast, sleeper Nos. 7, 8, and 16 were used for verification of a simple and efficient detection method per the use of a sound-level meter.

2.2 Bending test method

Figure 3 presents the scheme of a bending test focusing on the cross-sections at the rail seats of Sleeper Nos. 1 and 9. This scheme complies with Japanese Industrial

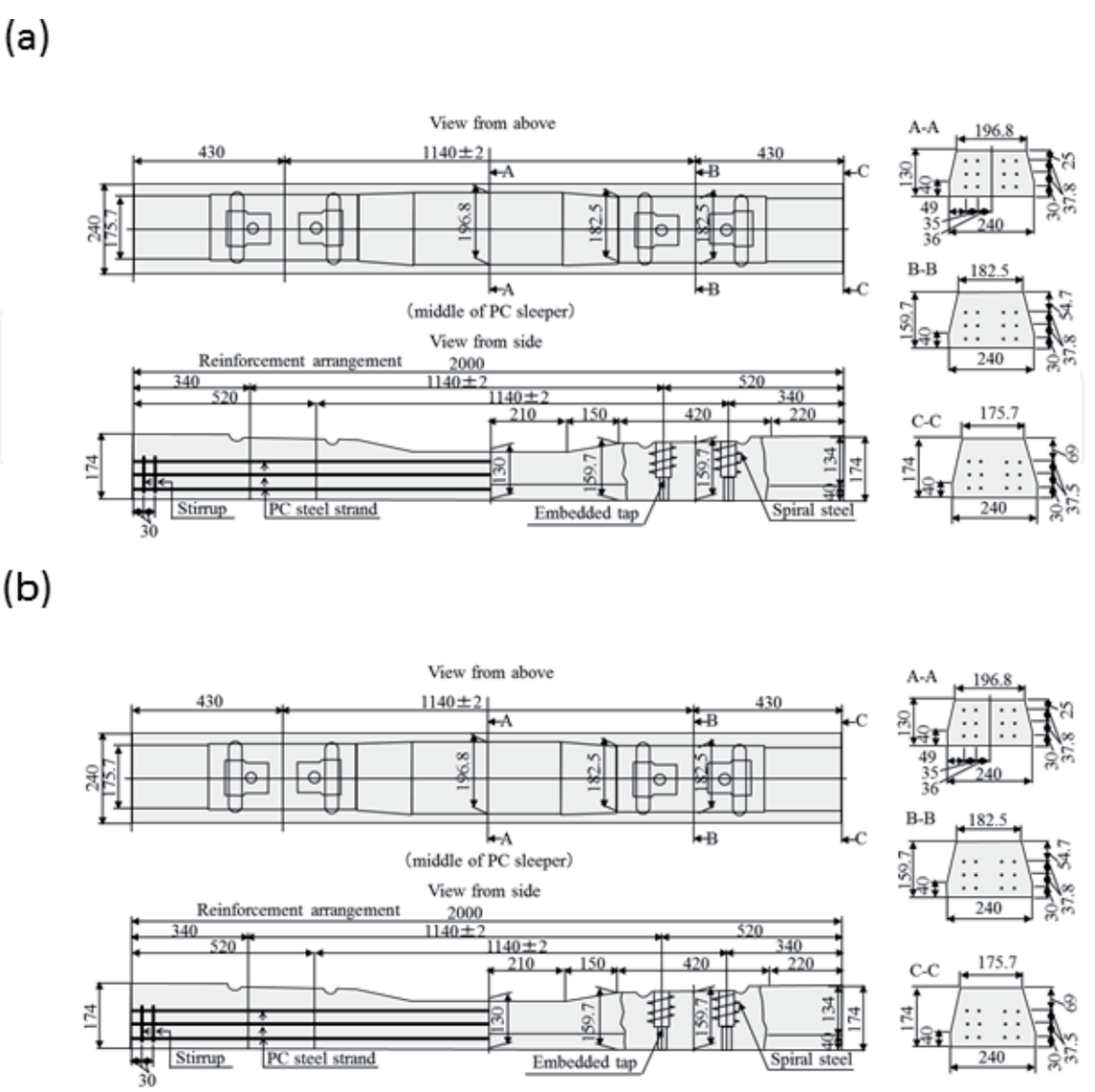

Figure 2.
Specifications of prestressed concrete sleeper on meter-gauged line prescribed in Japanese Industrial Standard: (a) the pretension type named 3PR and (b) the posttension type named 3PO.

	Cross section	A-A	B-B
3PR	Bending proof load	81 kN	50 kN
	Bending ultimate load	130 kN	86 kN
	Compressive strength	More than 49.1 N/mm²	
	Steel stranded wire	2.9 mm (3 stranded) × 12	
	Nominal elastic modulus of concrete	33.0 GPa	
	Concrete density	23.0 kN/m³	
	Cross section	A-A	B-B
3PO	Bending proof load	77 kN	45 kN
	Bending ultimate load	159 kN	92 kN
	Compressive strength	49.1N/mm² 以上	
	Steel lod	Nominal diameter 10 mm × 4	
	Nominal elastic modulus of concrete	33.0GPa	
	Concrete density	23.0kN/m³	

Table 1.
Nominal specifications of test concrete sleeper.

Standards E 1201 and 1202. In order to validate the impact of damage levels on modal characteristics, loading/unloading and vibration measurements were performed stepwise. Procedures for the bending test and the vibration measurement test are described as follows. First, a vibration measurement was performed in the intact state; second, vibration levels were measured after loading and unloading of the

Sleeper No.	Type	Test	Purpose	Damage level
1	3PR	I	Bending test	Intact Side Bottom
2	3PR	I	Actual damage	Crack at the bottom of RS (one side) Side Bottom
3	3PR	I	Actual damage	Cracks at the bottom of RS (both side) Side Bottom
4	3PR	I	Actual damage	Cracks at the bottom of RS (both side) Side Bottom
5	3PR	I	Actual damage	Cracks on whole area (Suspicion of ARS) Top Side Bottom
6	3PR	I	Ultimate state	After bending test of both rail and the middle position
7	3PR	III IV	Sound measuring	Broken at the bottom of RS and cracks (one side) Side face Bottom face
8	3PR	III IV	Sound measuring	Intact Side Bottom
9, 10	3PO	I	Bending test	Intact Side Bottom
11	3PO	I	Actual damage	Crack at the bottom of RS (one side) Side Bottom
12	3PO	I	Actual damage	Cracks at the bottom of RS (both side) Side Bottom
13	3PO	I	Actual damage	Cracks at the bottom of both RS and the top of middle (shown as whole area cracks) Top Side Bottom
14	3PO	I	Actual damage	Cracks on whole area and a steel rod fractured Side Bottom
15	3PO	I	Ultimate state	After bending test of both rail and the middle position
16	3PO	III IV	Sound measuring	Cracks at the bottom of RS (both side) Side Bottom
17–22	3PO	II	Other track member	Intact Side Bottom

* RS: Rail seat

Table 2.
List of collected concrete sleepers and associated damage levels.

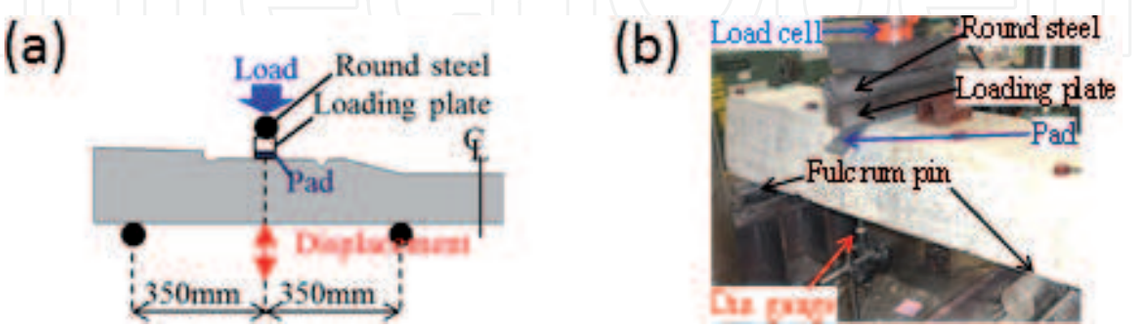

Figure 3.
Bending test scheme following the Japan Industrial Standards for concrete sleepers: (a) loading and supporting condition and (b) picture of installed concrete sleeper.

design-proof load; and third, after loading and unloading of the "cracking load," vibrational levels were again measured. The cracking load was determined by visual inspection which was conducted during the loading of this latter step. Subsequently,

after loading and unloading 1.2 times the cracking load observed in the last step, the vibration level was again measured. Finally, after loading and unloading of the "ultimate load," the resulting vibration levels were once again determined. The "ultimate load" is defined as the maximum load. Bending tests with these procedures were conducted for both cross sections of rail seats for concrete Sleeper Nos. 1 and 9.

2.3 Vibration and sound pressure test method

Table 3 provides the specifications of measurement equipment associated with this study. In order to identify vibration characteristics up to 1 kHz, all acceleration and sound pressure responses were recorded on a Laptop PC with a 5 kHz sampling rate via a preamplifier and an A/D converter. Accelerometers and sound-level meters were employed (models PV85 and NL62, Rion Co. LTD.) that have frequency ranges up to 7 and 20 kHz, respectively. Sound pressures were measured by a sound-level meter with a flat input window. An impulse hammer was adopted per PCB PREZORTONICS INC. model 086C03 with a 2.25 mV/N sensitivity load cell to excite up to a level of 1 kHz. The weight of the unit was 136 g. **Figure 4(a)** shows the observed input forces of the impulse hammer and indicates an overall relative flat-frequency response. **Figure 4(b)** represents the distribution of all input forces, with the average of the forces being 0.079 N.

Figure 5 describes the four vibration test methods and shows TEST I using 11 accelerometers in order to validate the impact of artificial or actual damage on mode characteristics of sleepers. Each concrete sleeper was supported by a soft urethane mattress of 600 mm thickness to simulate a free-free boundary condition [23]. TEST I was conducted on Sleeper Nos. 1–7 and 9–13. **Figure 5(b)** presents TEST II using nine accelerometers for the purpose of estimating the influences of other track members. TEST II was performed in a test line on the premises of the Railway Technical Research Institute, in which sleepers with two rails and rail pads were laid on ballast similar to an actual railway environment. Concrete Sleeper Nos. 17–22, all which were intact, were evaluated in TEST II.

Figure 5(c) and **(d)** presents TEST III and IV using two and one accelerometers and a single sound-level meter to validate the feasibility of an effective detection method. These tests were conducted on Sleeper Nos. 7, 8 and 16. TEST III and TEST IV adopted the supporting method via the use of a soft urethane mattress and ballast, respectively. TEST III also investigated the impact of other vibration modes, excitation points, and sound-level meter distances to investigate the optimal measurement method and to clarify the potential limitations of usage in practical applications. In all tests, free-vibration responses excited by an impulse hammer were measured. Impact forces were applied at the midspan (and at the rail seat for TEST III) of sleepers, with responses being recorded three separate times for the respective sleepers.

Instruments	Model	Corporation	Specifications
Piezoelectric acceleration meter	PV85	Rion Co., LTD.	Frequency range: 1–7000 Hz Charge sensitivity: 6.42 pC/(m/s^2)
Sound-level meter	NL-62	Rion Co., LTD.	Frequency range: 10–20000 Hz Frequency characteristic: Flat
Pre-amplifier	NH-22	Rion Co., LTD.	Frequency range: 10–100000 Hz
Impulse hammer	086C03	PCB PREZORTONICS INC.	Frequency range: 0–8000 Hz Hammer mass: 136 g
Data acquisition system	Ni cDAQ-9172 Ni9233 LabVIEW	National Instruments Japan Corporation	Sampling frequency: 5000Hz

Table 3.
Specifications of measurement equipment.

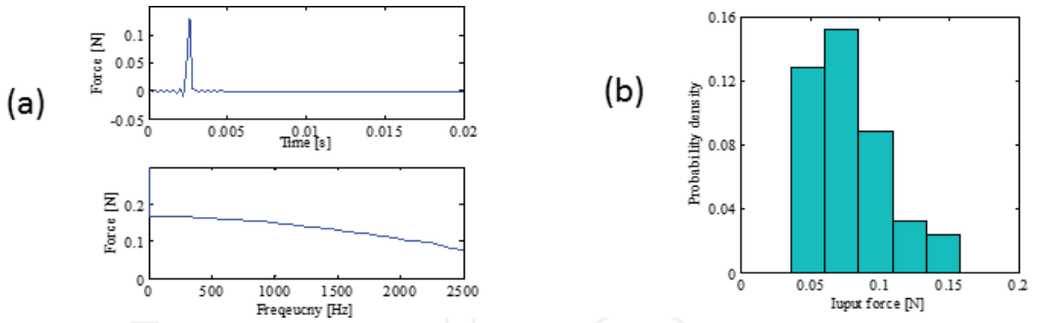

Figure 4.
Input force by impulse hammer: (a) time and frequency series and (b) distribution of input force.

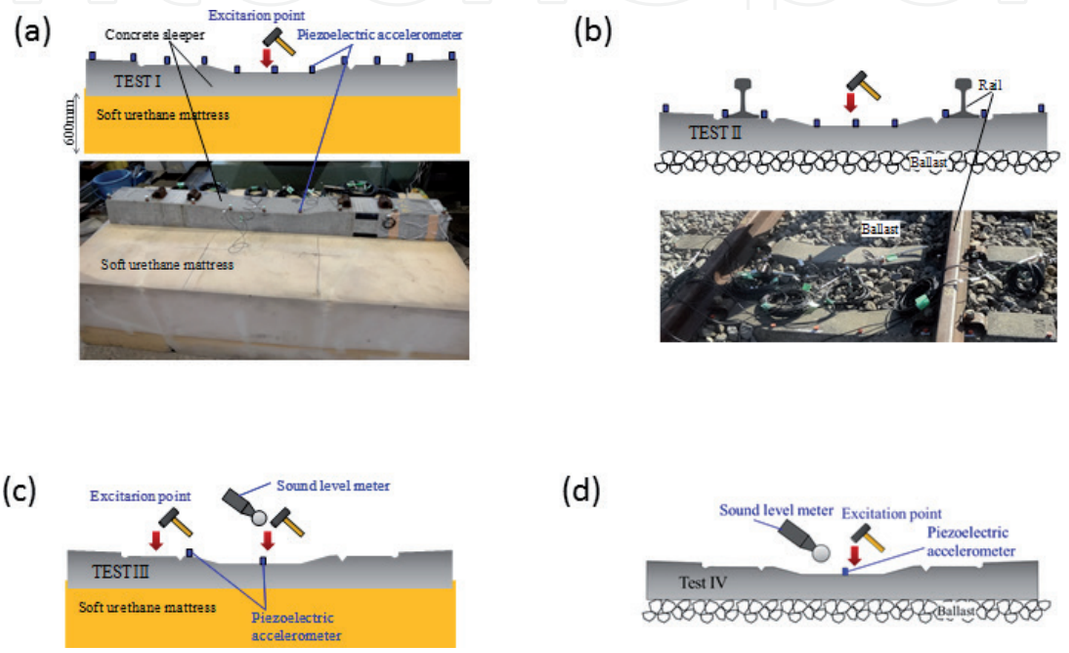

Figure 5.
Sensor arrangement and impact position of vibration and sound pressure test methods: (a) TEST I assuming free-free boundary condition; (b) TEST II assuming actual boundary condition; (c) TEST III assuming free-free boundary condition; and (d) TEST IV with ballast support.

2.4 Identification methods

Two well-known methods, ERA (Eigensystem Realization Algorithm) [23] and peak-picking were employed to identify the modal characteristics, natural frequency, modal damping ratio (ERA only), and modal shape (ERA only). Peak-picking was embedded into portable equipment for practical applications. Both identification methods, however, were neither capable of considering nonlinearity nor nonstationarity that may be caused by damage, such as breathing cracks. Several publications [24] have previously indicated that unsteady modal characteristics can express smaller structural damage scenarios. Concrete sleeper management, however, does not require the detection of such smaller-type damage events; being able to exclusively detect damaged sleepers that are in need of exchange is sufficient. Thus, this study adopted well-known time-invariant identification methods. As for ERA, more information about identification via the ERA method can be found in Refs. [25, 26]. Peak picking, which is the most simple and straightforward identification method for natural frequencies, was employed to develop an efficient detection system in the practical field. A 0.5-s acceleration just after impact excitation at the sleeper midspans was used for identification; thus, the resulting frequency increments were 2 Hz.

2.5 Numerical calculation method

In order to characterize the dynamics of concrete sleepers, many types of numerical models for concrete sleepers have been proposed. Grassie [5] proposed a simplified two-dimensional dynamic model in the free-free condition, with their analytical results having been verified by comparisons with 12 different types of sleepers. Dahlberg and Nielsen [27] developed a concrete sleeper model popularly denoted as the "Timoshenko Beam on an Elastic Foundation," for both free-free and in-situ conditions. Lam et al. [17, 18] also modeled the sleeper as a Timoshenko beam, the supporting ballast as discretized springs, and the rails as masses (with reference to previous studies [28, 29]). Furthermore, Kaewunruen and Remennikov [20] modeled the in-situ concrete sleeper as the sleeper, and the ballast and pads using the effective stiffness of the rails and pads.

In order to characterize affecting mechanisms of sleeper damage on modal characteristics, numerical calculations based on a finite-element model were performed in this study. **Figure 6** shows the subject numerical model for the concrete sleepers. Numerical analysis for the concrete sleepers was performed by LS-DYNA, version R8.0.0 [30]. A sleeper's concrete was modeled as hexahedral solid elements, and its steel wires and stirrups were modeled as beam elements. Supports and loading points for loading test analyses were modeled as rigid elements. A sleeper itself was modeled as a symmetrical model. Solid elements (concrete) and beam elements (steel wire and stirrups) share actual nodes to prevent slippage from occurring. **Table 4** shows the material properties of each element in the sleeper model. Young's modulus of concrete was set from the stress-strain curve. Uniaxial compression strength and uniaxial tensile strength of concrete was set from Young's modulus and Design Standards for Railway Structures and Commentary (Concrete Structures) [31]. For concrete, a material that can address cracking with tension softening and crushing was ultimately used [32]. Prestressing was reproduced by initial stress to the steel wires in the axial direction.

In order to reproduce the influence of bending damage upon modal characteristics, numerical simulations of loading and unloading under the same experimental bending conditions were first calculated, and then, the modal characteristics of damaged sleepers were investigated by eigenvalue analysis in each loading-unloading step.

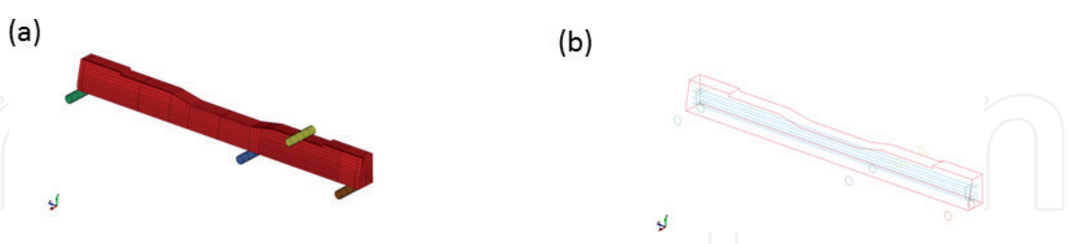

Figure 6.
Numerical model of a concrete sleeper: (a) finite-element of concrete and (b) reinforced steel.

Material	Element type	Young's modules (kN/mm^2)	Poisson's ratio	Density (kN/m^3)	Uniaxial compressive strength (kN/mm^2)	Uniaxial tensile strength (kN/mm^2)	Cross-sectional area (mm^2)	Initial tensile stresses (N/mm^2)
Concrete	solid	30	0.2	20	40	2.69	—	—
Steel wire (dia. 2.9 mm*3)	beam	200	0.3	77	—	—	19.82	1448
Strrup (dia. 4 mm)	beam	200	0.3	77	—	—	12.56	—

Table 4.
Element types and specifications of the numerical model.

3. Results

3.1 Bending test results

Figure 7 shows the load-displacement relationship at the rail seat, and **Table 5** shows applied loads of each state. In all cases, the cracking loads and ultimate loads were overdesign-proof and design-ultimate oriented. It can be confirmed that the bending of sleepers tends to soften gradually after the load exceeds cracking levels (i.e., around 110 kN). Both the cracking and ultimate loadings of Sleeper No. 9 in the posttension system are larger than those of Sleeper No. 1 in the pretension system. Although bending tests were performed at the right and left rail seats, explicit differences between the respective cases were not observed.

Figure 7, moreover, presents numerical calculation results. The results agree well with the experimental findings for pretension type Sleeper No. 1. A first crack occurred at the bottom of the rail seat as shown in **Figure 8**. The crack load is altogether depicted in **Table 5**, and the 112 kN cracking load agrees with the 111 kN

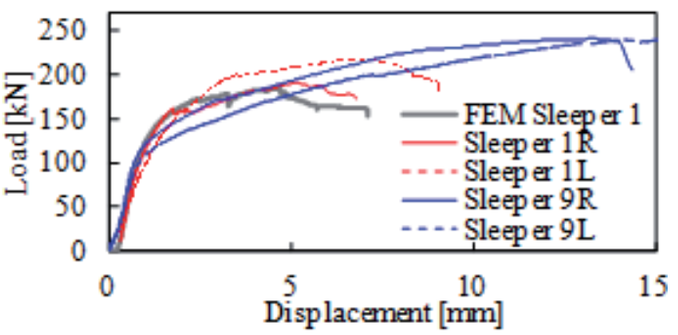

Figure 7.
Load-displacement envelope curve on bending test.

States	Applied loads [kN]				
	1R	1L	9R	9L	FEM
Undamaged	0	0	0	0	0
Design proof	81	81	77	77	81
Cracking	111	108	124	126	112
1.2 × cracking	133	130	149	151	134
Ultimate	190	215	240	245	184

(R: right side, L: left side)

Table 5.
Bending test results.

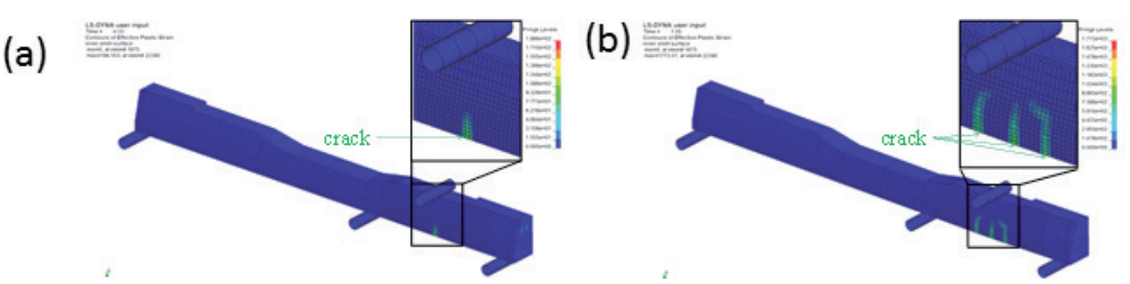

Figure 8.
Contours of cracks at (a) 112 kN and (b) 184 kN applied loads.

experimental result. For the ultimate state, three total cracks were found at the rail seat. This fracture mode is likewise consistent with the experimental one, as shown in **Figure 9**. Thus, it can be confirmed that the numerical model can accurately reproduce those realistically propagated in the damaged state.

Figure 10 shows the crack-width at the bottom of the rail seat calculated by the numerical model. **Figure 10(a)** indicates the general trend of prestressed concrete and that the maximum width of the first crack, crack 2, becomes wider with increasing load. In contrast, **Figure 10(b)** shows the residual crack-width after unloading. Residual cracks first appeared after an approximate 170 kN loading, which is close to the ultimate load. This means that most opened cracks due to such a loading can ultimately close back together after unloading, due to residual prestresses.

3.2 Modal identification results with bending tests

Figure 11 presents the time history and Fourier spectrum of measured accelerations at Sleeper No. 1 prior to the bending test. The vibrational measurements of Sleeper Nos. 1 and 9 (intact) were conducted based on TEST I, and the modal characteristics were identified by the ERA method.

Figure 12 shows the identified and numerically calculated natural frequencies and modal shapes from the first to third modes of Sleeper No. 1. These numerical results were calculated using the calibrated numerical model. The model displayed a value of 1.3 times that of the nominal elastic modulus for concrete based on the core

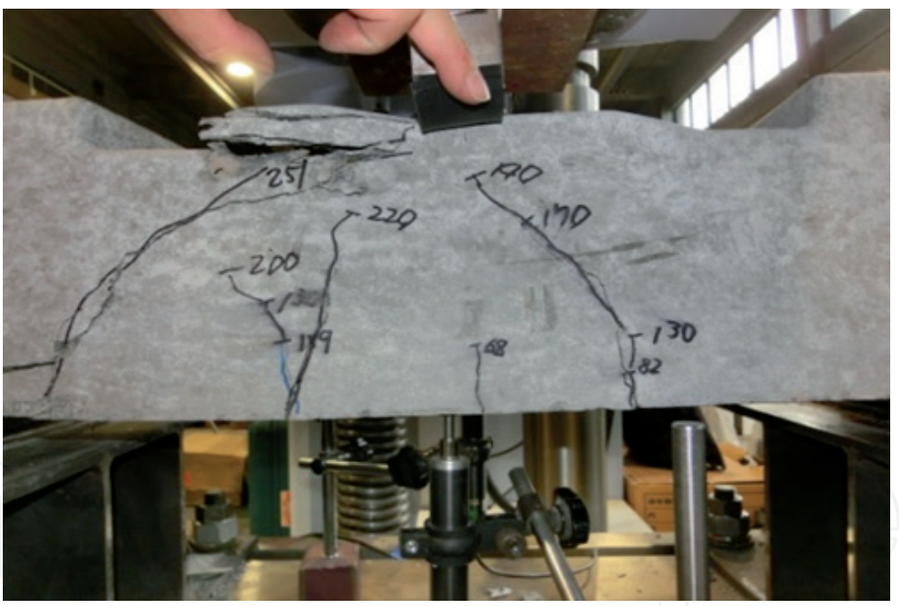

Figure 9.
Photograph of cracking at ultimate condition.

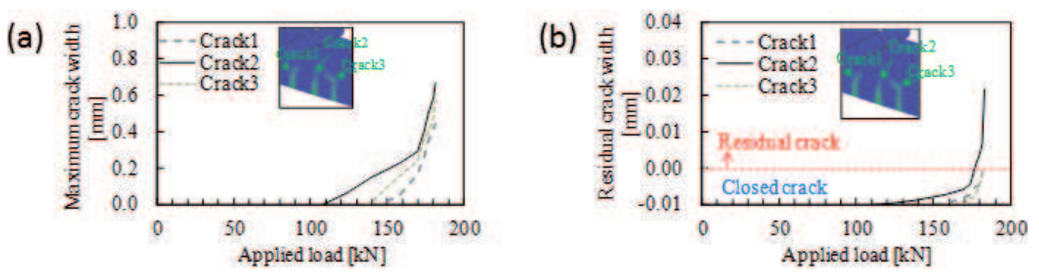

Figure 10.
Relationship between maximum applied load and crack width: (a) maximum crack width under load and (b) residual crack width after unloading.

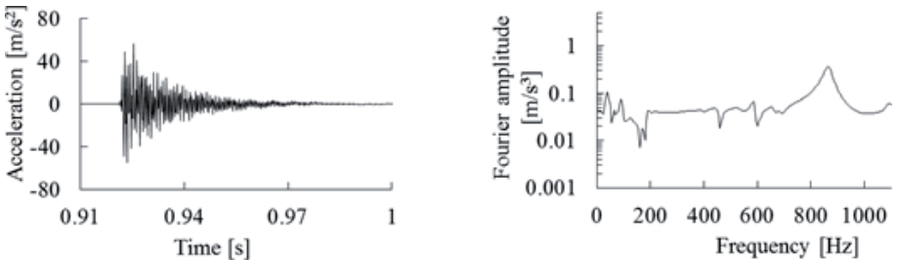

Figure 11.
Measured acceleration time history and spectrum on the midspan of Sleeper No. 1.

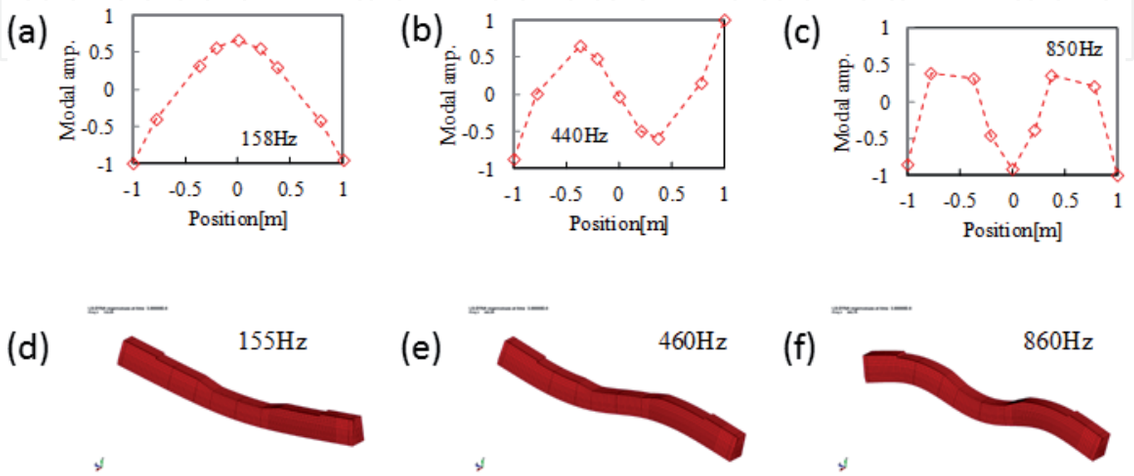

Figure 12.
Comparison of identified and calculated natural frequencies and mode shapes: (a)–(c) identified first-third bending mode; (d)–(f) calculated first-third bending mode of Sleeper No. 1.

test result of Sleeper No. 1. The numerical and identified natural frequencies and modal shapes showed good agreement within each mode.

3.3 Impact of applied loads on modal characteristics

Figures 13–15 show natural frequencies, modal damping ratios, and mode shapes of the first to third modes. These were identified by the ERA method using TEST I, which were conducted for each loading-unloading step. Numerical results, natural frequencies, and modal shapes, obtained by eigenvalue analysis, are shown in **Figures 13** and **15**.

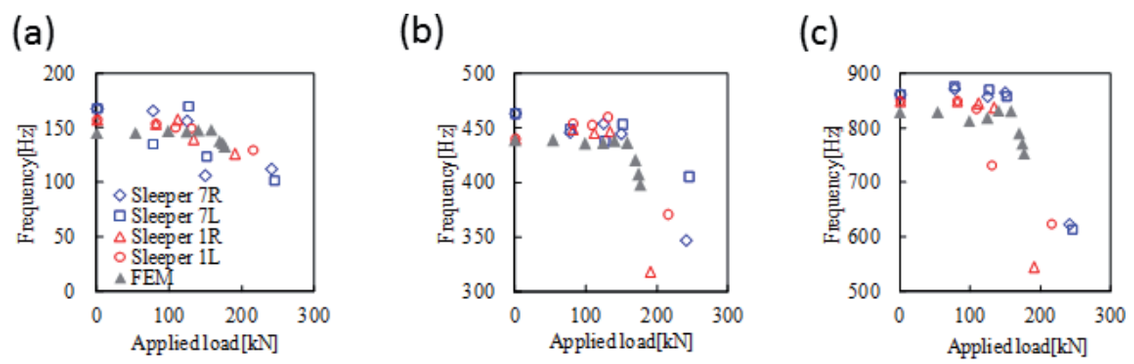

Figure 13.
Impact of applied load on natural frequency: (a) first bending mode; (b) second bending mode; and (c) third bending mode.

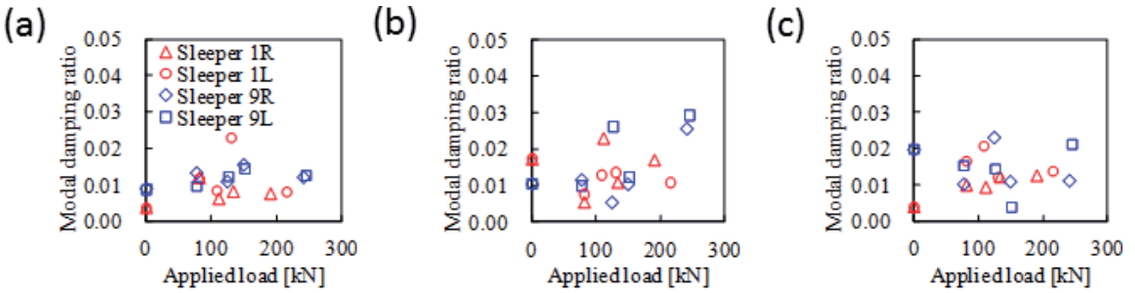

Figure 14.
Impact of applied load on modal damping ratio: (a) first bending mode; (b) second bending mode; and (c) third bending mode.

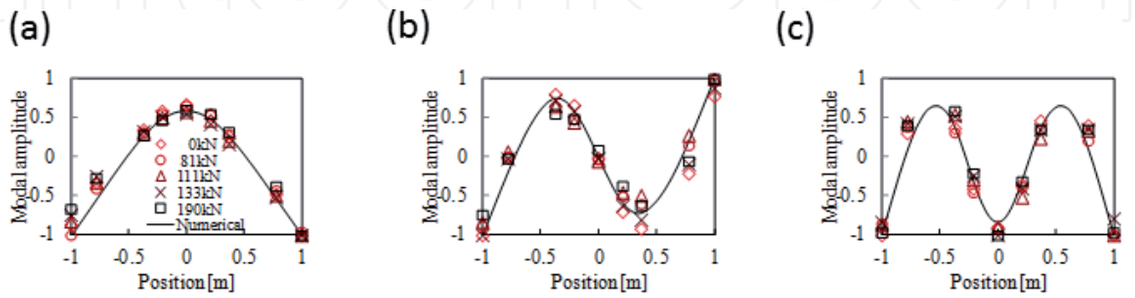

Figure 15.
The impact of applied load on right rail seat (−0.45 m position in each figure) and modal shape: (a) first bending mode; (b) second bending mode; and (c) third bending mode.

Figure 13 indicates that the natural frequency decreases rapidly when the applied load reaches a value of 1.2 times the cracking load (about 130 kN) or greater. This tendency is consistent with the numerical model when a concrete crack remains open even after unloading. Thus, it is perceived that a reduction in bending rigidity due to an open crack has a greater impact on a decrease in natural frequency than other bending-damage modes such as the plasticizing of steel rods or stranded wires, or reduction of introduced pretension. As shown in **Figure 13**, the natural frequency of the third mode in the ultimate state drops by approximately 150 Hz (17%) in all samples. It can therefore be asserted that the agreement of location between a crack generation and a higher modal amplitude might cause these large decreases in natural frequency within the third mode.

Figure 14 represents well-known large variations in mode-damping ratios. Some increasing tendencies of damping ratios due to increased applied loads can be seen in the first and second modes of Sleeper No. 9. Modal damping ratios are, however, difficult to apply as damage detection indicators due to a lack of certainty.

Figure 15 shows the modal shapes of Sleeper No. 1 from bending tests conducted at the left rail seat. It is typically difficult to find the impact of loading influences on modal shapes. If a modal shape is ultimately adapted as a detection indicator, another challenge would be at hand in which the use of numerous sensors would be required for carrying out multipoint measurements.

Figure 16 shows identified natural frequencies of concrete sleepers, in which damage has been generated during actual service. Vibration measurements were performed via TEST I on Sleeper Nos. 1–6 and 9–15 as shown in **Table 1**. Results of Sleeper Nos. 1 and 9 are representative of intact states prior to bending tests.

For the first mode frequency, some of the sleepers (e.g., Nos. 6 and 9) differ with the overall trend of decreasing frequency due to damage. The bending-tested Sleeper No. 6 and the intact Sleeper No. 9 have relatively high and low frequencies, respectively. Accordingly, it is not easy to detect damaged sleepers using first mode frequencies. With respect to the second mode, the frequencies of damaged sleepers

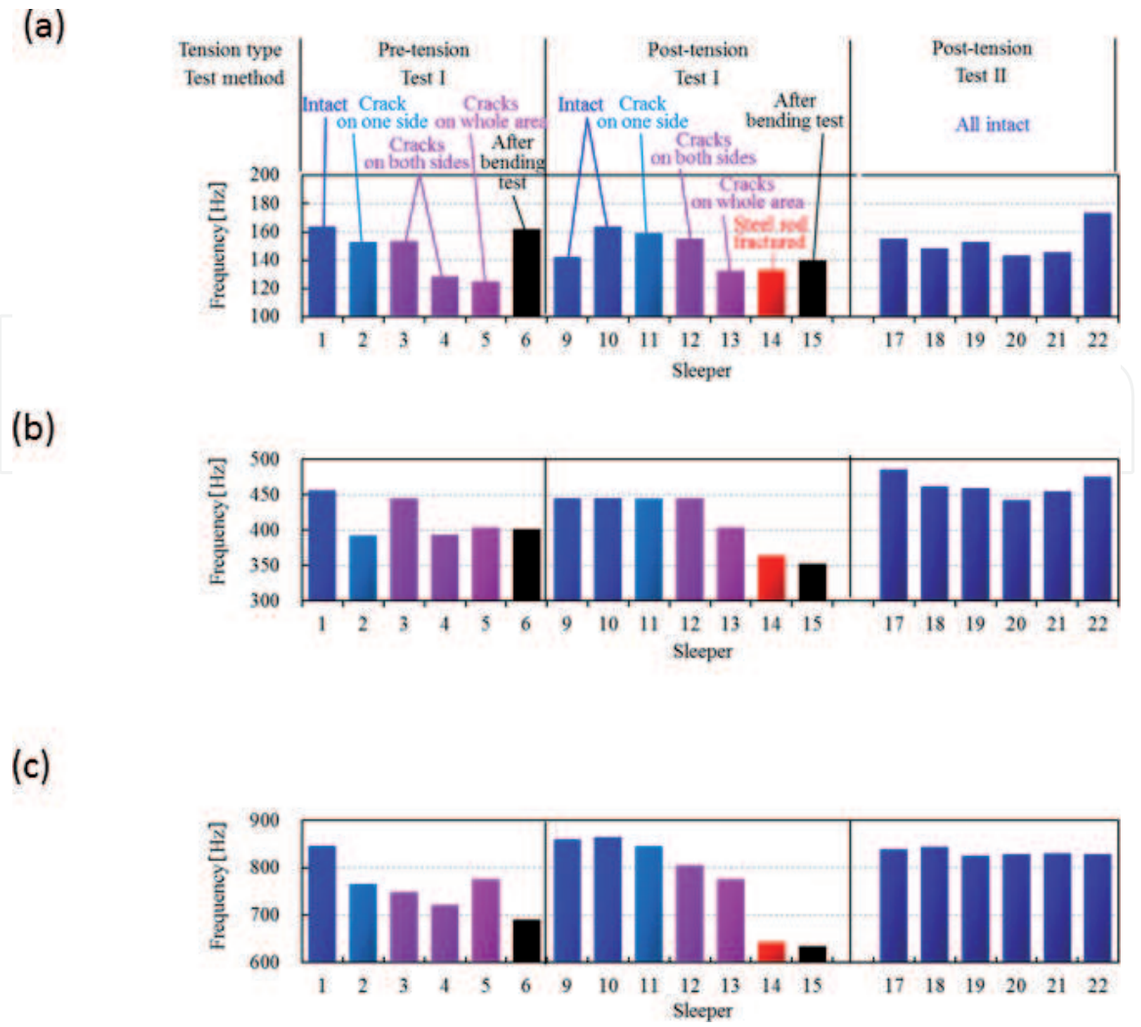

Figure 16.
Impact of actual damage and actual environment on natural frequency: (a) first bending mode; (b) second bending mode; and (c) third bending mode.

are low in comparison to those of intact ones. The natural frequencies of Sleeper No. 14 with a steel rod fracture and Sleeper Nos. 6 and 15 after postloading are significantly reduced. For the third mode, frequencies of damaged sleepers are clearly less compared with those of intact ones. In essence, the overall tendency seems to point to the notion that severity of damage typically corresponds to a proportional decrease in frequency. An inconsistency in this trend can be seen only in Sleeper No. 5 which has cracks in nearly all areas and yet exhibits a slightly higher frequency than that of less-damaged Sleeper No. 2. Sleeper Nos. 2 and 5, however, show sufficient declines in frequency to be able to clearly identify their relative levels of damage.

Thus, there were no hindrances to detect damaged sleepers when third bending frequencies were adopted as a detection index. Frequency-based damage detection is a well-known method based on simple concepts carried out through numerical analysis and laboratory tests; there are however, only limited examples of such application achievements within the civil structural domain. In response to this notion, this subject study strives to empirically validate the feasibility of a detection method using third bending mode frequency via experimental evaluation of actual damaged sleepers.

3.4 Impact of the actual environment on natural frequency

For operational railway tracks, concrete sleepers are laid on supporting ballast, along with two rails and pads. In particular, ballast-supporting stiffness has been

historically measured in large variations [33]. Thus, a superior detection indicator should not only be sensitive to damage but also "insensitive" to the states of other track members such as ballast and pads. In order to validate the feasibility of frequency-based damaged-sleeper detection in the actual field, potential impacts from the external environment were investigated. Vibration measurement TEST II and modal identification were hence conducted on intact concrete Sleeper Nos. 17–22, which were on a test line within Railway Technical Research Institute premises.

Figure 16 presents the identified natural frequencies of Sleeper Nos. 17–22. A large variation could be confirmed in the first and second bending modes. It can thus be asserted that the variation of specifications in other track members causes this large variation because completely intact concrete sleepers themselves all display the same properties. On the other hand, the variations in the third bending mode are small. These empirical results are consistent with the trends pointed out in the existing literature [22], in which the variation of ballast-supporting stiffness mainly affects low-order modes, such as first and second bending. These results therefore imply that the third bending mode frequency is a suitable detection indicator, which consistently exhibits desirable characteristics for efficient damaged-sleeper detection, as described above.

4. Discussion about the simplification

4.1 Applicability of peak picking

The applicability of peak picking, one of the simplest methods for identifying third bending mode frequencies, was investigated. A Fourier spectrum was created by a 0.5-s acceleration at the midspan of sleepers just after an impact excitation. Peak frequencies corresponding to the third bending mode were picked up from the range of 500–1000 Hz frequency according to the aforementioned results discussed in this study.

Figure 17 presents identified third bending mode frequencies by ERA and peak picking. Both sets of results show excellent agreement; thus, peak picking can effectively identify the third bending mode frequency (i.e., suitable detection indicator) based on a simple measurement using only a single accelerometer.

Figure 18 presents measured FFT spectra of three tests, which translates to a certain reliability level within the peak picking method. Peaks of three measured spectra were in good agreement for each test sleeper. It should be noted that only damaged Sleeper Nos. 3, 4, 12, and 14 have some minor peaks and discrepancies at frequency ranges other than the peaks between test cases. This complex influence might be caused by nonlinearity or nonstationarity due to damage; thus, there is some degree

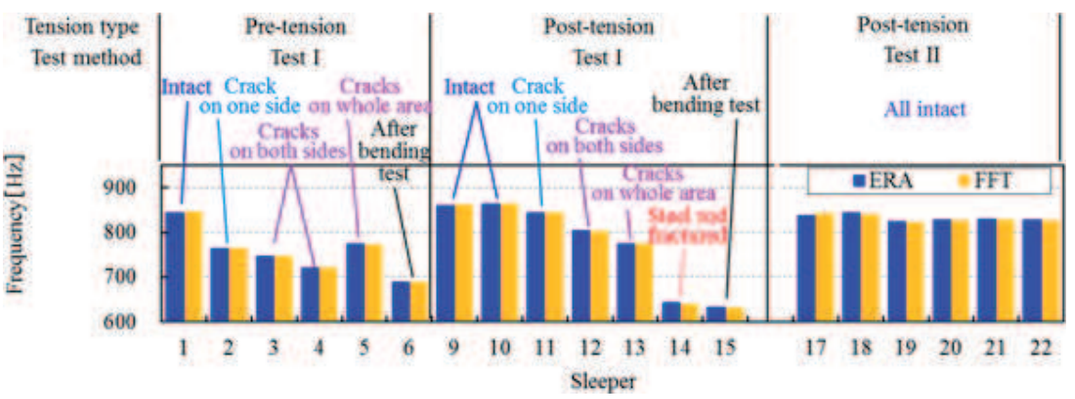

Figure 17.
Comparison of identification methods of third bending mode frequency based on TEST I and TEST II.

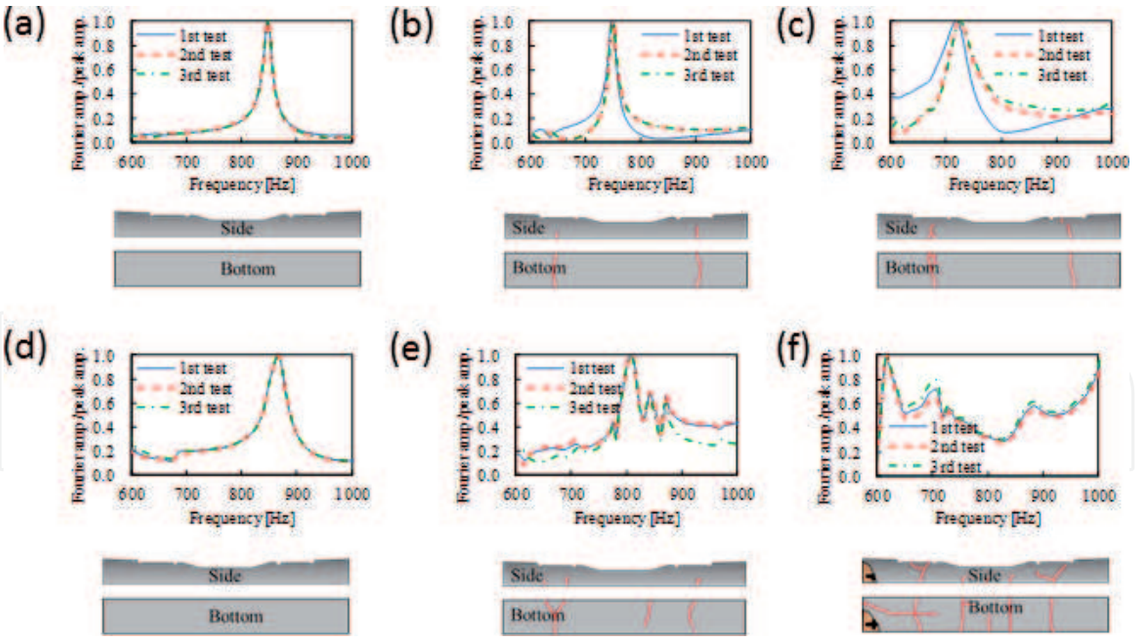

Figure 18.
Reliability of measured spectrum based on TEST I: (a) Sleeper No. 1; (b) Sleeper No. 3; (c) Sleeper No. 4; (d) Sleeper No. 9; (e) Sleeper No. 12; and (f) Sleeper No. 14.

of possibility that such damage can be detected by focusing on those influences. The peak frequency of concrete sleepers is, however, reduced because of damage and can be easily and reliably found by the peak picking method in the absence of information regarding nonlinearity or nonstationarity. Thus, it can be concluded that peak picking is sufficient for damaged concrete sleeper detection as maintained in this study.

4.2 Applicability of hammering sound

In the quest for additional simple measurement techniques, damage detection by sound-level meters that do not require the installation of accelerometers was experimentally investigated focusing on Sleeper Nos. 7, 8, and 16.

Structural vibrations can be propagated to peripheral regions as acoustic radiation via the air. Thus, sound pressure caused by impulse hummer test has possibility to be used for indirectly identification of concrete sleepers. Considering the modal characteristics and convenience of practical use, this study sets the sound-level meter position to above the midspan of the sleepers, which can match the antinode positions of the third bending modal shape. In addition, this feasibility study experimentally investigated the effect of each mode on measured sound pressure and then provided an optimized measurement method to ultimately obtain the third bending mode frequency of test sleepers to apply it for practical uses.

Figure 19 shows Fourier spectra of acceleration responses and sound pressure. The acceleration spectra at the midspan and near the rail seats of a sleeper, in addition to sound pressure, are depicted in the **Figure 19**. **Figure 19(a)** presents the results when an impulse hammer excitement occurs at the midspan, and **Figure 19(b)** corresponds to when the hammer is excited at the rail seat. **Figure 19** indicates good agreement between spectra of acceleration and sound pressure around the frequency peak corresponding to the third mode (750–800 Hz). This fact supports the applicability of sound pressure measurement as a robust tool for damaged-sleeper detection. Another peak of sound pressure(s) in the realm of 350–400 Hz corresponds to the accelerations not at the midspan, but exclusively at the rail seat. Thus, these peaks are caused by second bending vibrations of sleepers. The sound pressure can thus surveil not only the third mode but also the second mode. However, when comparing

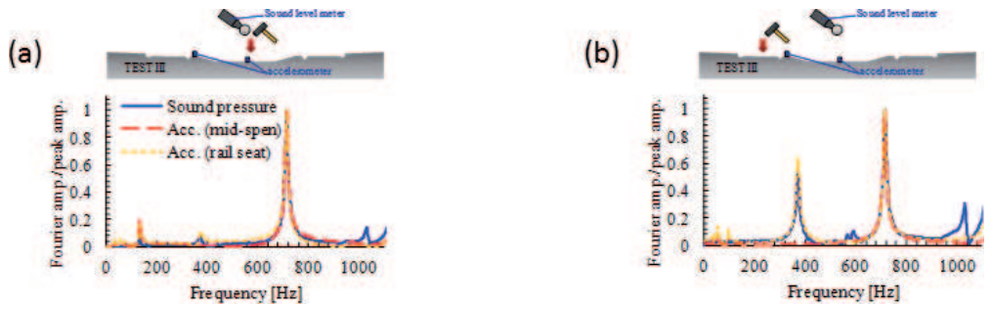

Figure 19.
Comparison between acceleration and sound pressure based on Fourier spectrum in TEST III: (a) Sleeper No. 7 with midspan excitation and (b) Sleeper No. 7 with rail seat excitation.

between midspan and rail seat excitation, the midspan excitation can ultimately reduce the second mode vibration level and hence make it easier to identify the third mode frequency by peak picking. It should be noted that the first mode (150–200 Hz) has little impact on the sound pressure because the vibration magnitude is significantly smaller than those of the second and third modes.

Figure 20(a) and **(b)** shows the impulse hammer test scheme to investigate the influence of sound observation positions. As shown in **Figure 20(a)**, the position of the sound-level meter was varied among 0.1, 0.3, and 0.5 m from the top surface of the sleeper. In addition, a convenient method of wearing the sound-level meter around the worker's neck (as shown in **Figure 20(c)**) was performed. The peak frequencies of the third mode for Sleeper No. 16 were extracted by peak picking. **Figure 20(d)** shows the extracted peak frequencies of measured acceleration and sound pressure corresponding to the third mode. It was confirmed that the peak frequency of sound pressure can estimate the third mode at the same value for all positions in this test and that these were consistent with the peak frequencies of

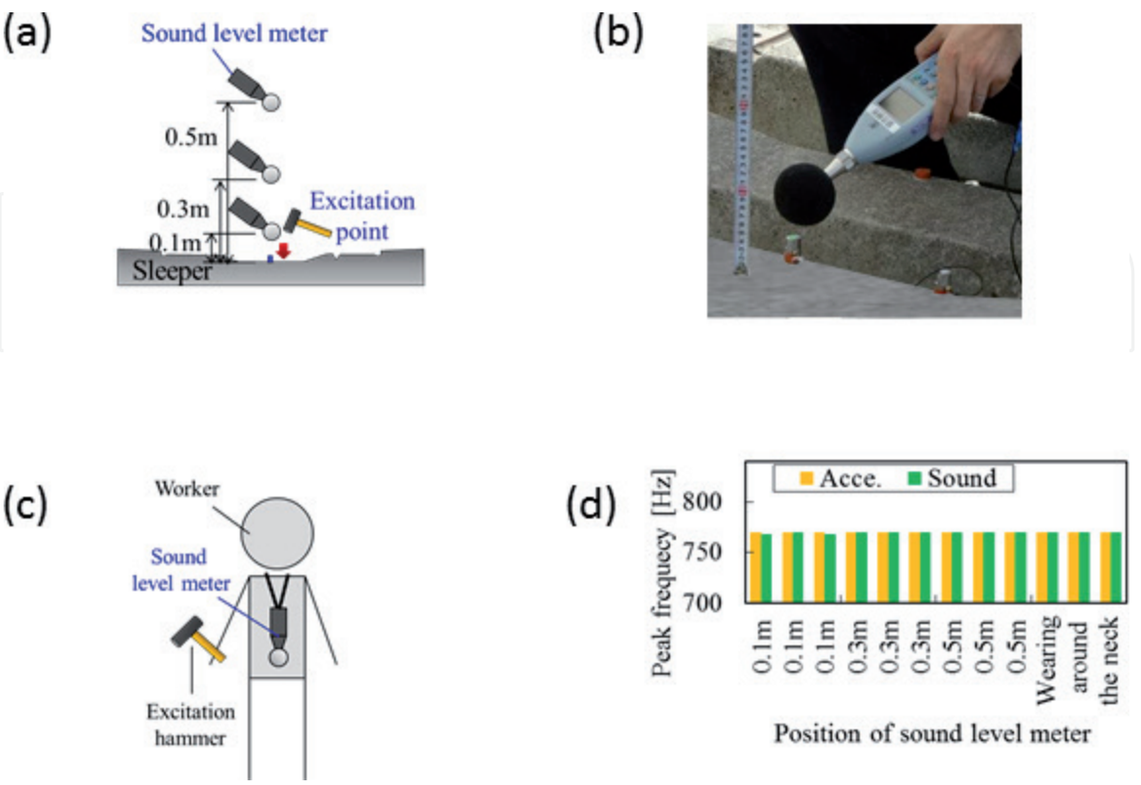

Figure 20.
Influence of distance of sound-level meter from excitation point: (a) test position; (b) example of sound-level meter condition; (c) wearing around the worker's neck and (d) comparison of peak frequencies.

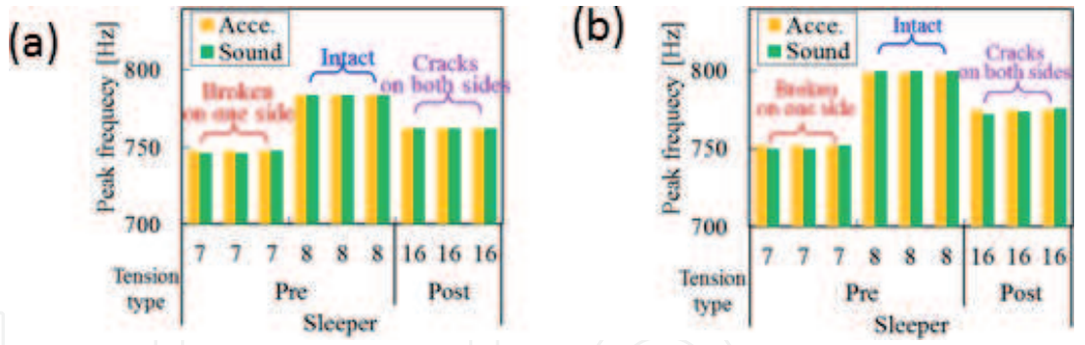

Figure 21.
Peak frequencies of acceleration and sound pressure based on (a) TEST III with support at both ends and (b) TEST IV with ballast support.

acceleration at the midspan. Thus, appropriate positioning of the sound-level meter is required to set it in the vicinity of the excitation point. **Figure 20(d)** illustrates that the same peak frequencies are obtained by a worker who performs an impulse excitation measurement by wearing a sound-level meter about the neck. This demonstrates an efficient damaged-sleeper detection protocol that can excite, measure, and provide a determination all via a single worker.

Figure 21(a) and **(b)** summarizes the peak frequencies of acceleration and sound pressure obtained based on TEST III and TEST IV, which were performed on concrete Sleeper Nos. 7, 8, and 16. The excitation points were at the sleeper midspans, and sound-level meters were worn around the worker's neck. Peak frequencies of acceleration and sound pressure were all found to be in good agreement. In addition, the peak frequency of damaged Sleeper No. 7 was clearly less than that of intact Sleeper No. 8 in both TEST III and IV. Therefore, it can be empirically verified that induced damages decrease frequencies within the third mode and that such frequencies can be accurately estimated via sound pressure measurements, even if the supporting method is changed to ballast (Test IV) from a soft urethane mattress.

5. Conclusions

In order to validate the feasibility of a frequency-based damage detection method, which is a well-known concept but has seen minimal practical application within the realm of railway concrete sleepers, this study experimentally investigated the impacts of artificial or actual damage on the modal characteristics of such sleeper. In addition, an efficient detection method based on sound pressure and its applicability for practical use was empirically validated. The associated resulting conclusions are summarized as follows:

1. Based on vibration measurements performed in parallel with bending tests, it was confirmed that natural frequencies start to be reduced when greater than 1.2 times the cracking load is applied.

2. Via numerical study, it was confirmed that reductions in natural frequency are caused by open cracks which remain open after unloading has occurred.

3. It was verified empirically that the natural frequency of the third mode (which is not only sensitive against damage but also less influenced by pad stiffness and ballast-supporting stiffness) is a suitable indicator for damaged-sleeper detection based on acceleration measurement tests of sleepers with actual damage and measurement tests on full-scale test lines.

4. Natural frequencies of third mode suitable for damage detection coincide with the peak frequencies of acceleration at the central sleeper segments, and, the peak frequency of acceleration matches the peak frequency of sound pressure measured by a noise meter. Thus, it became clear that it is possible to detect damaged sleepers via a noncontact measurement mode per the use of a sound-level meter.

5. As the results of investigation for the noncontact measurement method inherently assume a practical application, the protocol of wearing a sound-level meter around a worker's neck could suitably estimate the frequency of the third mode for concrete sleepers and altogether enable the efficient detection of damaged sleepers, including the likes of excitation, measurement, and determination by a singular worker.

When comparing the natural frequencies of the third mode obtained by the noncontact measurement techniques presented in this study, many deep damaged concrete sleepers can ultimately be detected from a large number of those measured. Furthermore, the proposed process can significantly contribute in the determination of sleeper-exchanging priorities according to the amount of measured frequency reduction in various cases.

Conflict of interest

There are no conflicts of interest to declare.

Author details

Kodai Matsuoka* and Tsutomu Watanabe
Railway Technical Research Institute Structural Mechanics in Railway Dynamics Division, Kokubunji-shi, Japan

*Address all correspondence to: matsuoka.kodai.13@rtri.or.jp

References

[1] FIP Commission on Prefabrication, FIP Commission on Prefabrication. Working Group on Concrete Railway Sleepers, Fédération Internationale de la Précontrainte. Working Group on Concrete Railway Sleepers. Concrete Railway Sleepers. Thomas Telford Services Ltd. One Great George Street, London, United Kingdom; 1987

[2] Remennikov A, Kaewunruen S. Experimental investigation on dynamic railway sleeper/ballast interaction. Experimental Mechanics. 2006;**46**(1):57-66. DOI: 10.1016/s0014-5793(01)03293-8

[3] Wakui H, Okuda H. A study on limit state design method for prestressed concrete sleepers. Doboku Gakkai Ronbunshu. 1997;**1997**(557):35-54. DOI: 10.2208/jscej.1997.557_35

[4] Yun WY, Ferreira L. Prediction of the demand of the railway sleepers: A simulation model for replacement strategies. International Journal of Production Economics. 2003;**81**:589-595. DOI: 10.1016/S0925-5273(02)00299-2

[5] Grassie SL. Dynamic modelling of concrete railway sleepers. Journal of Sound and Vibration. 1995;**187**(5): 799-813. DOI: 10.1006/jsvi.1995.0564

[6] Gustavson R. Structural Behaviour of Concrete Railway Sleepers. Göteborg, Sweden: Chalmers University of Technology; Sweden; 2002

[7] Kaewunruen S, Remennikov A. Post-Failure Mechanism and Residual Load-Carrying Capacity of Railway Prestressed Concrete Sleeper Under Hogging Moment. North Melbourne, Australia: The Institute of Materials Engineering Australasia; 2006

[8] Kaewunruen S, Remennikov AM. Dynamic crack propagations in prestressed concrete sleepers in railway track systems subjected to severe impact loads. Journal of Structural Engineering. 2009;**136**(6):749-754. DOI: 10.1061/(ASCE)ST.1943-541X.0000152

[9] Dukkipati RV, Dong R. Impact loads due to wheel flats and shells. Vehicle System Dynamics. 1999;**31**(1):1-22. DOI: 10.1076/vesd.31.1.1.2097

[10] Barke D, Chiu WK. Structural health monitoring in the railway industry: A review. Structural Health Monitoring. 2005;**4**(1):81-93. DOI: 10.1177/1475921705049764

[11] Salawu OS. Detection of structural damage through changes in frequency: A review. Engineering Structures. 1997;**19**(9):718-723. DOI: 10.1016/S0141-0296(96)00149-6

[12] Johnson EA, Lam HF, Katafygiotis LS, Beck JL. Phase I IASC-ASCE structural health monitoring benchmark problem using simulated data. Journal of Engineering Mechanics. 2004;**130**(1):3-15. DOI: 10.1061/(ASCE)0733-9399(2004)130:1(3)

[13] Sohn H, Farrar CR, Hemez FM, Shunk DD, Stinemates DW, Nadler BR, et al. A Review of Structural Health Monitoring Literature: 1996-2001. USA: Los Alamos National Laboratory; 2003. DOI: 10.1.1.729.3993

[14] Rice JA, Spencer BF Jr. Flexible Smart Sensor Framework for Autonomous Full-Scale Structural Health Monitoring. Newmark Structural Engineering Laboratory. Champaign, IL, USA: University of Illinois at Urbana-Champaign; 2009. DOI: 10.12989/sss.2010.6.5_6.423

[15] Siringoringo DM, Fujino Y. Observed dynamic performance of the Yokohama-Bay bridge from system identification using seismic records. Structural Control and Health

Monitoring. 2006;**13**(1):226-244. DOI: 10.1002/stc.135

[16] Dilena M, Morassi A. Dynamic testing of a damaged bridge. Mechanical Systems and Signal Processing. 2011;**25**(5):1485-1507. DOI: 10.1016/j.ymssp.2010.12.017

[17] Lam HF, Hu Q, Wong MT. The Bayesian methodology for the detection of railway ballast damage under a concrete sleeper. Engineering Structures. 2014;**81**:289-301. DOI: 10.1016/j.engstruct.2014.08.035

[18] Lam HF, Wong MT, Yang YB. A feasibility study on railway ballast damage detection utilizing measured vibration of in situ concrete sleeper. Engineering Structures. 2012;**45**:284-298. DOI: 10.1016/j.engstruct.2012.06.022

[19] Kaewunruen S, Remennikov A. Application of Vibration Measurements and Finite Element Model Updating for Structural Health Monitoring of Ballasted Railtrack Sleepers With Voids and Pockets. New York, United States: Mechanical Vibration: Measurement, Effect, and Control, Nova Science Publishers; 2009

[20] Kaewunruen S, Remennikov AM. Effect of improper ballast packing/tamping on dynamic behaviors of on-track railway concrete sleeper. International Journal of Structural Stability and Dynamics. 2007;7(01):167-177. DOI: 10.1142/S0219455407002174

[21] Kaewunruen S, Remennikov AM. Sensitivity analysis of free vibration characteristics of an in situ railway concrete sleeper to variations of rail pad parameters. Journal of Sound and Vibration. 2006;**298**(1-2):453-461. DOI: 10.1016/j.jsv.2006.05.034

[22] Matsuoka K, Watanabe T, Minoura S, Sogabe M, Omodaka A. Vibration modes of damaged PC sleepers and development of a simple damage detection method using sound level meter. Journal of Japan Society of Civil Engineers, Ser. E2 (Materials and Concrete Structures). 2018;**74**:158-175. DOI: 10.2208/jscejmcs.74.158

[23] Juang JN, Pappa RS. An eigensystem realization algorithm for modal parameter identification and model reduction. Journal of Guidance, Control, and Dynamics. 1985;**8**(5):620-627. DOI: 10.2514/3.20031

[24] Douka E, Hadjileontiadis LJ. Time–frequency analysis of the free vibration response of a beam with a breathing crack. NDT and E International. 2005;**38**(1):3-10. DOI: 10.1016/j.ndteint.2004.05.004

[25] Nagayama T, Abe M, Fujino Y, Ikeda K. Structural identification of a nonproportionally damped system and its application to a full-scale suspension bridge. Journal of Structural Engineering. 2005;**131**(10):1536-1545. DOI: 10.1061/(ASCE)0733-9445(2005)131:10(1536)

[26] Matsuoka K, Kaito K, Watanabe T, Sogabe M. Identification of dynamic properties of open-deck viaducts under passing train loads. In: Civil Engineering Topics. Vol. 4. New York, NY: Springer; 2011. pp. 155-162. DOI: 10.1007/978-1-4419-9316-8_13

[27] Dahlberg T, Nielsen J. Dynamic Behaviour of Free-Free and In-Situ Concrete Railway Sleepers. London, United Kingdom: Chalmers University of Technology, Solid Mechanics, Services Ltd; 1991

[28] Ford R. Modal analysis of a concrete railway sleeper. In: Research Note AVG/RN881122-1, School of Mechanical and Industrial Engineering. Australia: UNSW; 1988

[29] Vincent G. Modal analysis and numerical modeling of a concrete railway sleepers [Master of Engineering thesis]. Göteborg, Sweden: Department of Structural Engineering, Chalmers University of Technology; 2001

[30] Hallquist JO. LS-DYNA Keyword User's Manual 970. Livermore, CA, United States: Livermore Software Technology Corporation; 2007. pp. 299-800

[31] Design RS. Design Standards for Railway Structures and Commentary (Concrete Structures). Tokyo: Railway Technical Research Institute; 2007

[32] Grassl P, Xenos D, Nyström U, Rempling R, Gylltoft K. CDPM2: A damage-plasticity approach to modelling the failure of concrete. International Journal of Solids and Structures. 2013;**50**(24):3805-3816. DOI: 10.1016/j.ijsolstr.2013.07.008

[33] Esveld C. Modern Railway Track. 2nd ed. Delft, Netherlands: Delft University of Technology; 2001